Channel Characteristics Comparison of Single-Relay and Two-Relay Two-Way PLC Systems

Angie A. G. Liong *, Lenin Gopal *, Filbert H. Juwono *, Choo W. R. Chiong *, and Yue Rong †
* Department of Electrical and Computer Engineering, Curtin University Malaysia, 98009 Miri, Sarawak, Malaysia
†Department of Electrical and Computer Engineering, Curtin University, Perth WA 6845, Australia
Email: angie.liong@postgrad.curtin.edu.my, {lenin, filbert.hilman, raymond.ccw}@curtin.edu.my, y.rong@curtin.edu.au

***Abstract*—Power line communications (PLC) is one of the preferred technology for smart grid communication. Recent works have shown that the performance of the system improved with the aid of relay nodes. However, many PLC applications need two-way communication links where the channels are highly correlated to each other. For this reason, two-relay two-way PLC channel system become more desirable. In this paper, we aim to model the two-relay PLC forward and backward channel transfer functions (CTFs) using ABCD matrix. We also investigate the channel characteristics by comparing the CTFs between single-relay and two-relay two-way PLC systems. It is shown that for non-direct links, the CTFs of the two systems are comparable. However, single-relay systems have better direct link CTFs compared to the ones of two-relay systems.**

***Index Terms*—Channel characteristics, power line communications (PLC), two-way PLC system, single-relay, two-relay, forward channels, backward channels**

I. Introduction

The research on power-lines as the means for information delivery started in the late 1990's. Ever since then, power-line communication (PLC) technology has been popular for data transmission for indoor and outdoor data communication as power-line infrastructure is available widely [1]–[3]. With the high power demand and the introduction of successful deployment toward achieving the smart grid system, it can meet the demand of the higher data-transmission rate [4], [5].

PLC systems can be designed to be more reliable and advanced through the understanding of power-line channel characteristics. In fact, there are a number of research works on the power-line channel modelling to facilitate PLC research. Of all channel modelling approaches, the bottom-up approach is preferred as it represents the topology of the power-line network. It is performed by implementing the transmission line (TL) theory to obtain the channel transfer function (CTF) using the network information [6]–[8]. In addition, this approach is convenient to characterize power-line channels with relay(s). Relaying makes data transmission more reliable in long distance communication systems [9].

A single-relay, or sometimes called as three-nodes, one-way channel model has been proposed in [10]. However, many PLC applications need two-way communication links. In [11], the system performance of two-way relay-aided PLC was evaluated. Furthermore, an extended channel model of the one in [10] for two-way scheme relay-aided PLC was presented in [12]. It has been shown that the links in the two-way channels are highly correlated to each other. Additionally, the channel transfer functions (CTFs) of the forward and backward channels have been shown to be different.

It is obvious that the performance of the system can be further improved by adding more relays. In particular, it has been shown that the average capacity, coverage, and throughput improve with the increase of the number of relays [13], [14]. However, increasing the number of relays increases the total power consumption due to the static power of modem [15].

A bottom-up channel model for two-relay one-way PLC network has been derived in [14]. It has been found that in two-relay system, the use of both relays degrades the channel transfer function (CTF) when compared to the use of one relay only. It has been stated that the physical topology affects the channel characteristics [16]. Therefore, when we need to opt for using single-relay or two-relay two-way PLC system, we need to observe the channel characteristics for both systems. Nevertheless, the comparison of channel transfer function of single-relay and two-relay two-way PLC system is not available in the literature. This paper fills this gap by first extending the one-way channel model in [14] into two-way channel model. Next, we deploy a few comparable topologies and scenarios and simulate their CTFs.

The remaining of this paper is organised as follows. Section II discusses the two-relay two-way PLC channel topology. CTFs for two-relay PLC forward and backward channels are shown and derived. Numerical examples are given in Section III to verify the result. Finally, the main conclusion of work are highlighted in Section IV.

II. Two-Relay Two-Way PLC Channel Topology

In this paper, we use Canate's hybrid point-to-point (P2P) channel model which consists of four segments and three branches, where each branch is terminated by a load impedance [17]. In each segment, the cable is characterized by its parameters and length. For the sake of simplicity and fairness, we assume that the three terminated loads have the same impedances.

A general channel model of a two-branch transmission circuit consists of five cascaded two-port sub-circuits, i.e. three backbone transmission line segments, Φ_1, Φ_3, Φ_5, and two branched-circuit segments, Φ_2, Φ_4, is depicted in Fig. 1. Further, Fig. 2 shows the two-port network layout of the proposed two-relay PLC system model consisting of source (S), relay 1 (R_1), relay 2 (R_2), and destination (D). Its simplification along with the possible communication links is shown in Fig. 3.

We first obtain the equivalent input impedance which depends on cable types, parameters, and lengths. Next, the equivalent impedance is used to obtain the ABCD matrix of each segment. The overall ABCD matrix for the whole structure is the product of the ABCD matrix of each segment. Using the overall ABCD matrix, the transfer function can be obtained and expressed as the ratio of the load voltage to the source voltage [18], [19]. The composite CTF for a certain link can be found by summing the respective CTFs of the segments which constitute the link. For example, the composite CTF of the entire S-R_1-D link is the sum of CTF of S-R_1 segment and CTF of R_1-D

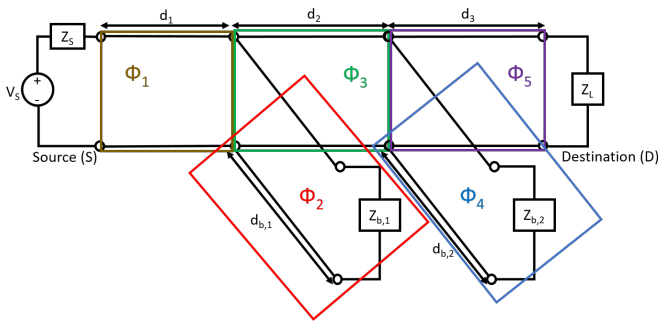

Fig. 1. A transmission line with two-branch circuit

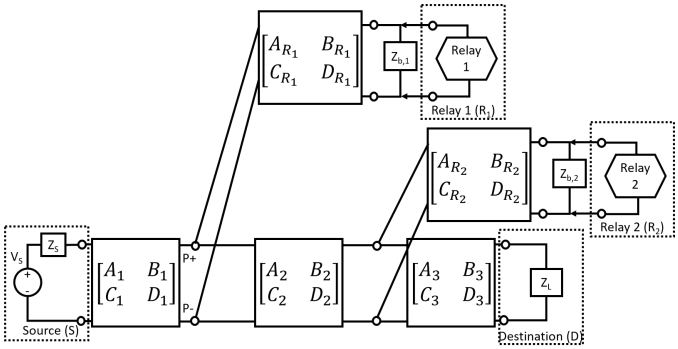

Fig. 2. Network layout of segment

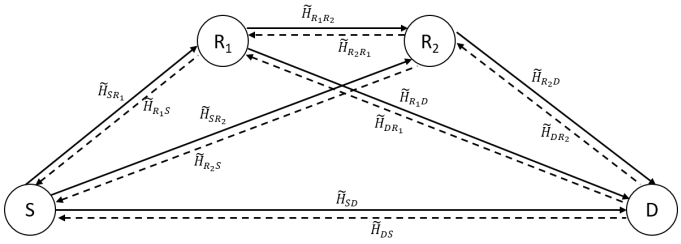

Fig. 3. A four-node two-way system model

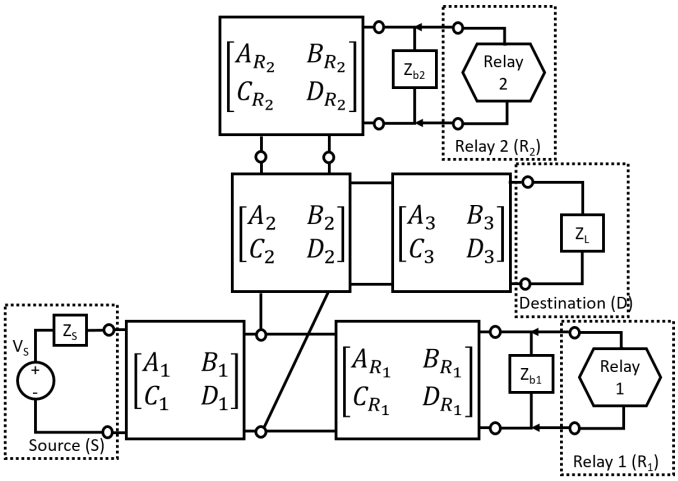

Fig. 4. Network layout of the path S to R_1

segment. If amplify-and-forward (AF) relay is used, we will have an amplifying constant in each segment except the last ABCD matrix [14].

A. CTFs for Two-Relay PLC Forward Channels

The steps for obtaining the forward CTFs are explained as follows. Due to the page limitation, we just present the CTF for S - R_1 - D link as an example. Other CTFs can be obtained through similar steps. Interested readers may read [14] for the details.

- We divide the path into two, i.e. S to R_1 and R_1 to D. From the S - R_1 point of view, R_2 and D behave as branches. Similarly, from the R_1 - D point of view, R_2 and S behave as branches.
- We consider the path S - R_1 as in Fig. 4. First, we calculate the branch impedance where R_2 is parallel to D. The equivalent input impedance of the branch is calculated by the impedance sum of R_2 and D, given by

$$Z_{R_2D} = \frac{A_2 Z'_{R_2D} + B_2}{C_2 Z'_{R_2D} + D_2}, \tag{1}$$

where Z'_{R_2D} is the equivalent impedance of $Z_{eq2}||Z_{Deq}$, Z_{eq2} is the equivalent input impedance of R_2, and Z_{Deq} is the equivalent impedance of the D branch. Their expressions are given by

$$Z'_{R_2D} = Z_{eq2}||Z_{Deq} = \frac{Z_{eq2}Z_{Deq}}{Z_{eq2} + Z_{Deq}}, \tag{2}$$

$$Z_{eq2} = \frac{A_{R_2} Z'_{LR_2} + B_{R_2}}{C_{R_2} Z'_{LR_2} + D_{R_2}}, \tag{3}$$

$$Z'_{LR_2} = Z_{b_2}||Z_{LR_2} = \frac{Z_{b_2} Z_{LR_2}}{Z_{b_2} + Z_{LR_2}}, \tag{4}$$

$$Z_{Deq} = \frac{A_3 Z_L + B_3}{C_3 Z_L + D_3}. \tag{5}$$

Second, we get the ABCD matrix of the direct path from S to R_1 as follows

$$\Phi^{(1)}_{SR_1} = \begin{bmatrix} A^{(1)}_{SR_1} & B^{(1)}_{SR_1} \\ C^{(1)}_{SR_1} & D^{(1)}_{SR_1} \end{bmatrix} = \begin{bmatrix} 1 & Z_S \\ 0 & 1 \end{bmatrix} \begin{bmatrix} A_1 & B_1 \\ C_1 & D_1 \end{bmatrix} \begin{bmatrix} 1 & 0 \\ \frac{1}{Z_{R_2D}} & 1 \end{bmatrix} \begin{bmatrix} A_{R_1} & B_{R_1} \\ C_{R_1} & D_{R_1} \end{bmatrix}$$

Third, the CTF of S - R_1 can be calculated by

$$H^{(1)}_{SR_1} = \frac{Z'_{LR_1}}{A^{(1)}_{SR_1} Z'_{LR_1} + B^{(1)}_{SR_1} + C^{(1)}_{SR_1} Z_S Z'_{LR_1} + D^{(1)}_{SR_1} Z_S}, \tag{6}$$

where Z'_{LR_1} is given by

$$Z'_{LR_1} = Z_{b_1}||Z_{LR_1} = \frac{Z_{b_1} Z_{LR_1}}{Z_{b_1} + Z_{LR_1}}. \tag{7}$$

- We consider the path R_1 - D as in Fig. 5. Similarly, we first calculate the equivalent impedance of S and R_2. Since the input impedance of R_2 is calculated earlier, the branch impedance of S can be expressed as

$$Z_{Seq} = \frac{A_1 Z_S + B_1}{C_1 Z_S + D_1}. \tag{8}$$

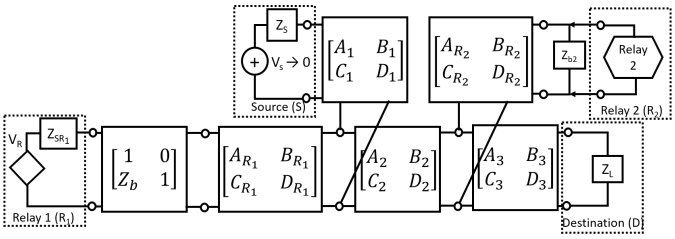

Fig. 5. Network layout of the path R_1 to D

Next, we get the ABCD matrix for R_1 - D as follows

$$\begin{aligned}\Phi_{R_1D}^{(2)} &= \begin{bmatrix} A_{R_1D}^{(2)} & B_{R_1D}^{(2)} \\ C_{R_1D}^{(2)} & D_{R_1D}^{(2)} \end{bmatrix} \\ &= \begin{bmatrix} 1 & 0 \\ Z_b & 1 \end{bmatrix} \begin{bmatrix} A_{R_1} & B_{R_1} \\ C_{R_1} & D_{R_1} \end{bmatrix} \begin{bmatrix} 1 & 0 \\ \frac{1}{Z_{Seq}} & 1 \end{bmatrix} \\ &\times \begin{bmatrix} A_2 & B_2 \\ C_2 & D_2 \end{bmatrix} \begin{bmatrix} 1 & 0 \\ \frac{1}{Z_{eq2}} & 1 \end{bmatrix} \begin{bmatrix} A_3 & B_3 \\ C_3 & D_3 \end{bmatrix}\end{aligned}$$

Third, the CTF of R_1 - D is given by

$$H_{R_1D}^{(2)} = \frac{Z_L}{A_{R_1D}^{(2)} Z_L + B_{R_1D}^{(2)} + C_{R_1D}^{(2)} Z_L Z'_{LR_1} + D_{R_1D}^{(2)} Z'_{LR_1}}. \tag{9}$$

- Lastly, the composite path gain of the entire S - R_1 - D link is given by

$$H_{SD}^{(R_1)} = (H_{SR_1}^{(1)} A) + H_{R_1D}^{(2)}, \tag{10}$$

where A is the amplification factor when AF relay is employed.

B. CTFs for Two-Relay PLC Backward Channels

Our remaining task is to derive the CTFs of the reverse links of the two-relay PLC system shown in Fig. 3.

1) Transfer function of the direct path from D to S: Considering the direct path from destination to source, the relay nodes, R_1 and R_2 are treated as the loads. The signaling of the direct path can be found by first calculating the equivalent impedance of the two relay branches as follows

$$Z_{eqb,1} = \frac{A_{R_1} Z'_{LR_1} + B_{R_1}}{C_{R_1} Z'_{LR_1} + D_{R_1}}, \tag{11}$$

$$Z_{eqb,2} = \frac{A_{R_2} Z'_{LR_2} + B_{R_2}}{C_{R_2} Z'_{LR_2} + D_{R_2}}. \tag{12}$$

Therefore, the matrix of the direct path from D to S is given by

$$\begin{aligned}\Phi_{DS}^{(D)} &= \begin{bmatrix} A_{DS}^{(D)} & B_{DS}^{(D)} \\ C_{DS}^{(D)} & D_{DS}^{(D)} \end{bmatrix} \\ &= \begin{bmatrix} A_3 & B_3 \\ C_3 & D_3 \end{bmatrix} \begin{bmatrix} 1 & 0 \\ \frac{1}{Z_{eqb,2}} & 1 \end{bmatrix} \begin{bmatrix} A_2 & B_2 \\ C_2 & D_2 \end{bmatrix} \\ &\times \begin{bmatrix} 1 & 0 \\ \frac{1}{Z_{eqb,1}} & 1 \end{bmatrix} \begin{bmatrix} A_1 & B_1 \\ C_1 & D_1 \end{bmatrix}.\end{aligned} \tag{13}$$

As a result, the CTF of the direct path from D to S can be expressed as

$$H_{DS}^{(D)} = \frac{Z_S}{A_{DS}^{(D)} Z_S + B_{DS}^{(D)} + C_{DS}^{(D)} Z_S Z_L + D_{DS}^{(D)} Z_L}. \tag{14}$$

2) Transfer function of the path D to S through R_1: This section describes the connection between two paths, i.e. D to R_1 and R_1 to S. When the signal travels from D to R_1, as always, R_1 is considered as the destination while S and R_2 behave as branches. The equivalent input impedance of the source branch is given by

$$Z_{eqb,3} = \frac{A_1 Z_S + B_1}{C_1 Z_S + D_1}. \tag{15}$$

Combining with the second relay impedance and the source impedance, the path matrix from D to R_1 can be expressed as

$$\begin{aligned}\Phi_{DR_1}^{(1)} &= \begin{bmatrix} A_{DR_1}^{(1)} & B_{DR_1}^{(1)} \\ C_{DR_1}^{(1)} & D_{DR_1}^{(1)} \end{bmatrix} \\ &= \begin{bmatrix} A_3 & B_3 \\ C_3 & D_3 \end{bmatrix} \begin{bmatrix} 1 & 0 \\ \frac{1}{Z_{eqb,2}} & 1 \end{bmatrix} \begin{bmatrix} A_2 & B_2 \\ C_2 & D_2 \end{bmatrix} \\ &\times \begin{bmatrix} 1 & 0 \\ \frac{1}{Z_{eqb,3}} & 1 \end{bmatrix} \begin{bmatrix} A_{R_1} & B_{R_1} \\ C_{R_1} & D_{R_1} \end{bmatrix},\end{aligned} \tag{16}$$

Therefore, the CTF for D - R_1 path is

$$H_{DR_1}^{(1)} = \frac{Z'_{LR_1}}{A_{DR_1}^{(1)} Z'_{LR_1} + B_{DR_1}^{(1)} + C_{DR_1}^{(1)} Z'_{LR_1} Z_L + D_{DR_1}^{(1)} Z_L}. \tag{17}$$

For the path from R_1 to S, R_1 behaves as the source and S behaves as the destination while R_2 and D become the branches. The equivalent input impedance of the destination branch is calculated through the impedance sum of R_2 and D as follows

$$Z_{eqb,4} = \frac{A_2 Z'_{R_2D} + B_2}{C_2 Z'_{R_2D} + D_2}, \tag{18}$$

where Z'_{R_2D} and $Z_{eqb,5}$ are respectively given by

$$Z'_{R_2D} = Z_{eqb,2} || Z_{eqb,5} = \frac{Z_{eqb,2} Z_{eqb,5}}{Z_{eqb,2} + Z_{eqb,5}}, \tag{19}$$

$$Z_{eqb,5} = \frac{A_3 Z_L + B_3}{C_3 Z_L + D_3}. \tag{20}$$

The path matrix for R_1 - S path is

$$\begin{aligned}\Phi_{R_1S}^{(2)} &= \begin{bmatrix} A_{R_1S}^{(2)} & B_{R_1S}^{(2)} \\ C_{R_1S}^{(2)} & D_{R_1S}^{(2)} \end{bmatrix} \\ &= \begin{bmatrix} 1 & 0 \\ Z_{b_1} & 1 \end{bmatrix} \begin{bmatrix} A_{R_1} & B_{R_1} \\ C_{R_1} & D_{R_1} \end{bmatrix} \begin{bmatrix} 1 & 0 \\ \frac{1}{Z_{eqb,4}} & 1 \end{bmatrix} \begin{bmatrix} A_1 & B_1 \\ C_1 & D_1 \end{bmatrix},\end{aligned}$$

Therefore, the CTF for R_1 - S path can be expressed as

$$H_{R_1S}^{(2)} = \frac{Z_S}{A_{R_1S}^{(2)} Z_S + B_{R_1S}^{(2)} + C_{R_1S}^{(2)} Z_S Z'_{LR_1} + D_{R_1S}^{(2)} Z'_{LR_1}}. \tag{21}$$

Finally, the composite path gain of the entire D - R_1 - S link is given by

$$H_{DS}^{(R_1)} = (H_{DR_1}^{(1)} A) + H_{R_1S}^{(2)}. \tag{22}$$

3) Transfer function of the path D to S through R_2: Using similar method, link D to S through R_2 consists of 2 paths, i.e. D - R_2 path and R_2 - S path. For the first path, S and R_1 are considered as branches. The equivalent input impedance of the S - R_1 branch is

$$Z_{eqb,6} = \frac{A_2 Z'_{SR_1} + B_2}{C_2 Z'_{SR_1} + D_2}, \tag{23}$$

where Z'_{SR_1} is given by

$$Z'_{SR_1} = Z_{eqb,1} || Z_{eqb,3} = \frac{Z_{eqb,1} Z_{eqb,3}}{Z_{eqb,1} + Z_{eqb,3}}. \tag{24}$$

The path matrix from D to R_2 is

$$\begin{aligned} \Phi^{(1)}_{DR_2} &= \begin{bmatrix} A^{(1)}_{DR_2} & B^{(1)}_{DR_2} \\ C^{(1)}_{DR_2} & D^{(1)}_{DR_2} \end{bmatrix} \\ &= \begin{bmatrix} A_3 & B_3 \\ C_3 & D_3 \end{bmatrix} \begin{bmatrix} 1 & 0 \\ \frac{1}{Z_{eqb,6}} & 1 \end{bmatrix} \begin{bmatrix} A_{R_2} & B_{R_2} \\ C_{R_2} & D_{R_2} \end{bmatrix}, \end{aligned} \tag{25}$$

Therefore, the CTF for D - R_2 path is

$$H^{(1)}_{DR_2} = \frac{Z'_{LR_2}}{A^{(1)}_{DR_2} Z'_{LR_2} + B^{(1)}_{DR_2} + C^{(1)}_{DR_2} Z'_{LR_2} Z_L + D^{(1)}_{DR_2} Z_L}. \tag{26}$$

In the second path, R_1 and D become the branches. The matrix for R_2 - S path is given by

$$\begin{aligned} \Phi^{(2)}_{R_2S} &= \begin{bmatrix} A^{(2)}_{R_2S} & B^{(2)}_{R_2S} \\ C^{(2)}_{R_2S} & D^{(2)}_{R_2S} \end{bmatrix} \\ &= \begin{bmatrix} 1 & 0 \\ Z_{b_2} & 1 \end{bmatrix} \begin{bmatrix} A_{R_2} & B_{R_2} \\ C_{R_2} & D_{R_2} \end{bmatrix} \begin{bmatrix} 1 & 0 \\ \frac{1}{Z_{eqb,5}} & 1 \end{bmatrix} \\ &\times \begin{bmatrix} A_2 & B_2 \\ C_2 & D_2 \end{bmatrix} \begin{bmatrix} 1 & 0 \\ \frac{1}{Z_{eqb,1}} & 1 \end{bmatrix} \begin{bmatrix} A_1 & B_1 \\ C_1 & D_1 \end{bmatrix} \end{aligned} \tag{27}$$

Therefore, the CTF for R_2 - S path is

$$H^{(2)}_{R_2S} = \frac{Z_S}{A^{(2)}_{R_2S} Z_S + B^{(2)}_{R_2S} + C^{(2)}_{R_2S} Z_S Z'_{LR_2} + D^{(2)}_{R_2S} Z'_{LR_2}}. \tag{28}$$

As usual, the path gain of the entire D - R_2 - S link is given by

$$H^{(R_2)}_{DS} = (H^{(1)}_{DR_2} A) + H^{(2)}_{R_2S}. \tag{29}$$

4) Transfer function of the path from D to S through R_1 - R_2: The link consists of three paths, i.e. D to R_2, R_2 to R_1, and R_1 to S. The equivalent input impedance for D to R_2 and R_1 to S have been derived earlier. Therefore, the matrix for R_2 - R_1 path is

$$\begin{aligned} \Phi^{(2)}_{R_2R_1} &= \begin{bmatrix} A^{(2)}_{R_2R_1} & B^{(2)}_{R_2R_1} \\ C^{(2)}_{R_2R_1} & D^{(2)}_{R_2R_1} \end{bmatrix} \\ &= \begin{bmatrix} 1 & 0 \\ Z_{b_2} & 1 \end{bmatrix} \begin{bmatrix} A_{R_2} & B_{R_2} \\ C_{R_2} & D_{R_2} \end{bmatrix} \begin{bmatrix} 1 & 0 \\ \frac{1}{Z_{eqb,5}} & 1 \end{bmatrix} \\ &\times \begin{bmatrix} A_2 & B_2 \\ C_2 & D_2 \end{bmatrix} \begin{bmatrix} 1 & 0 \\ \frac{1}{Z_{eqb,3}} & 1 \end{bmatrix} \begin{bmatrix} A_{R_1} & B_{R_1} \\ C_{R_1} & D_{R_1} \end{bmatrix} \end{aligned} \tag{30}$$

As a result, the CTF for R_2 - R_1 path is

$$H^{(2)}_{R_2R_1} = \frac{Z'_{LR_1}}{A^{(2)}_{R_2R_1} Z_{R_1} + B^{(2)}_{R_2R_1} + C^{(2)}_{R_2R_1} Z'_{LR_1} Z'_{LR_2} + D^{(2)}_{R_2S} Z'_{LR_2}}. \tag{31}$$

The composite path gain of the entire D - R_2 - R_1 - S link is expressed as

$$H^{(R_2R_1)}_{DS} = (H^{(1)}_{DR_2} A) + (H^{(2)}_{R_2R_1} A) + H^{(2)}_{R_1S}. \tag{32}$$

III. Numerical Results

For simulations, we assume the source has inner impedance of 50Ω and each terminated load (of R_1, R_2, and D) has the impedance of 150Ω. Note that the load impedance is commonly larger than the source impedance. The amplification factor, A is assumed to be 1. In this section, we present two simulations.

In Simulation 1, we present the segment and link CTFs of the two-relay two-way PLC. The PLC channel realization parameters for Simulation 1 are given in Table I. Each signalling path in the relay-involved channel is treated as an equivalent P2P channel. Using Canete's PLC channel simulator, the transfer function can be obtained as shown in Fig. 6. The summation of the respective CTFs of the segment can get the desired composite CTF as shown in Fig. 7. It can be seen that attenuation is higher in high frequencies.

TABLE I
Channel Realization Parameters

Line section	Length	Cable type	Terminated load
Backbone 1	$d_1 = 46.1m$	$n_{d_1} = 4$	N/A
Branch-tap 1	$d_{b,1} = 11.7m$	$n_{d_{b,1}} = 1$	$Z_1(f,T)$
Backbone 2	$d_2 = 39.6m$	$n_{d_2} = 3$	N/A
Branch-tap 2	$d_{b,2} = 23.5m$	$n_{d_{b,2}} = 2$	$Z_2(f,T)$
Backbone 3	$d_3 = 44.6m$	$n_{d_3} = 5$	N/A
Branch-tap 3	$d_{d,3} = 0$	N/A	$Z_{b,3} = \infty$
Backbone 4	$d_4 = 0$	N/A	N/A

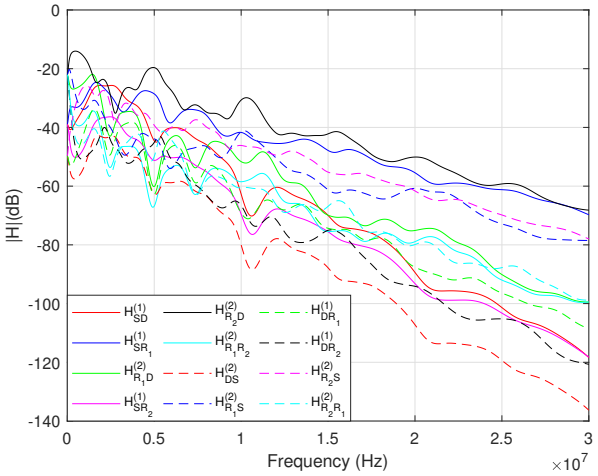

Fig. 6. CTFs of a two-relay two-way PLC system

In Simulation 2, we compare the link CTFs of single-relay two-way PLC system (SYS A) and two-relay two-way PLC system (SYS B). For the sake of fair comparison, we design

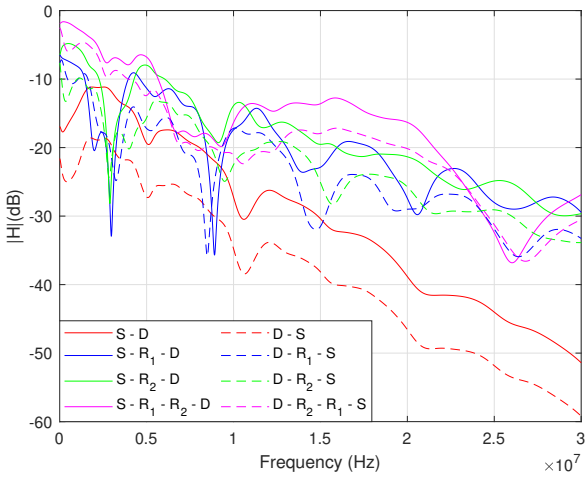

Fig. 7. CTFs for two-relay PLC forward and backward channels

four topologies and scenarios in Fig. 8 to observe the channel characteristics for both systems. Note that we use the same cable type for all segments here. We compare the link CTF when only one relay is used. In the first and second scenario, we compare the CTFs of the S - R - D and D - R - S links of the two systems. SYS B uses only one of its relays, either R_1 or R_2. We place the relay in SYS A according to the respective SYS B relay position to see the effect of the idle relay in SYS B. In scenario 3, we observe the CTF of the S - R_1 - R_2 - D and D - R_2 - R_1 - S links in SYS B. To make the comparison as fair as possible, we place the relay in SYS A at the midpoint of R_1 - R_2 distance. Lastly, scenario 4 compares the CTFs of SYS A and SYS B for their direct S - D and D - S links.

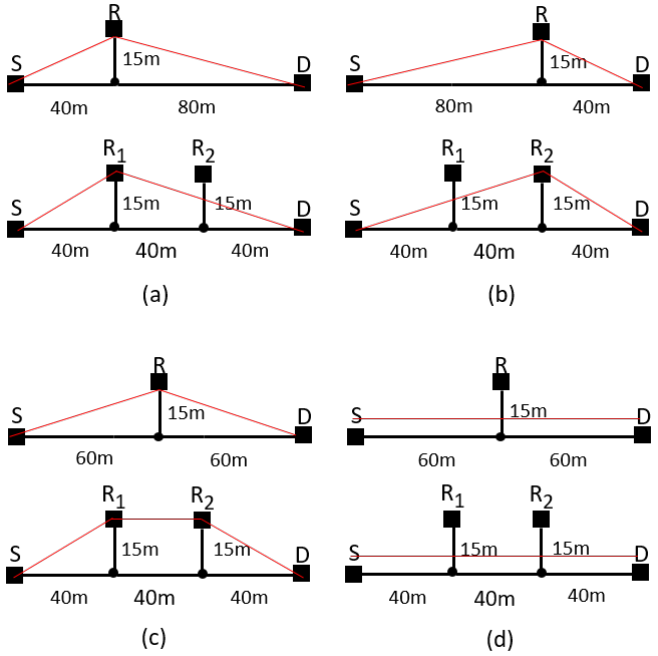

Fig. 8. Topologies for comparing two-way PLC systems with single relay and two relays: (a) scenario 1, (b) scenario 2, (c) scenario 3, and (d) scenario 4.

The simulation results of the four topologies are compared and depicted in Fig. 9. It can be seen that all forward channels give relatively better CTFs compared to the backward channels as the load impedance is larger than the source impedance.

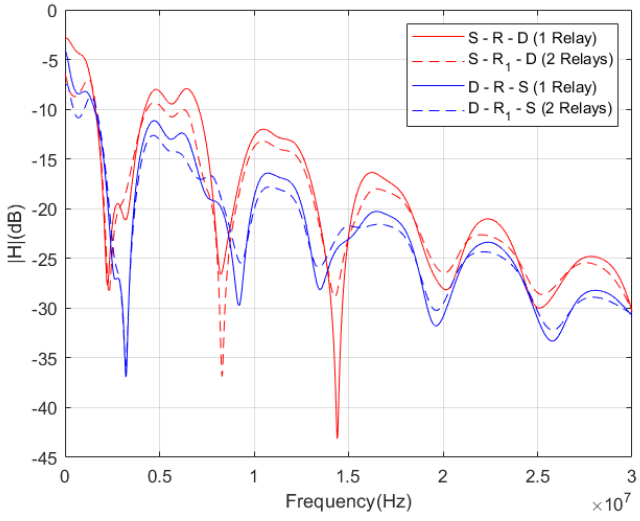

(a)

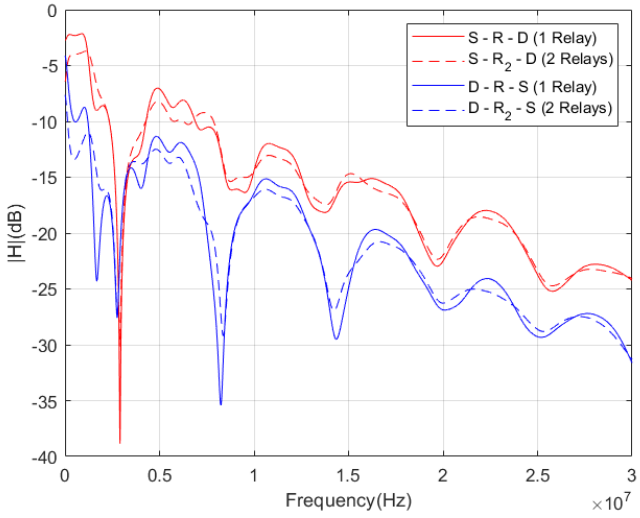

(b)

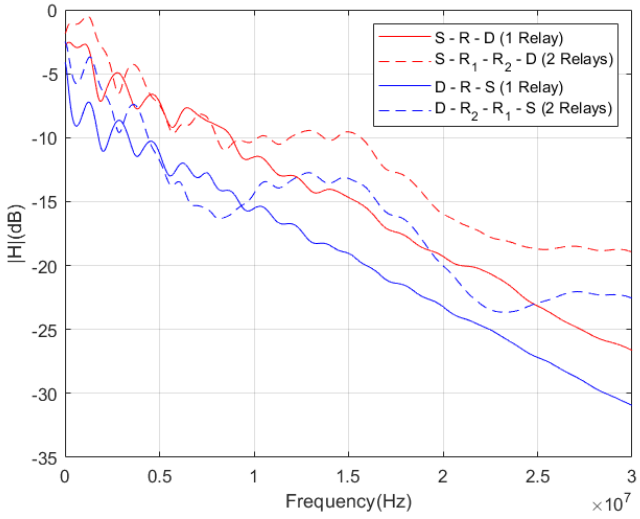

(c)

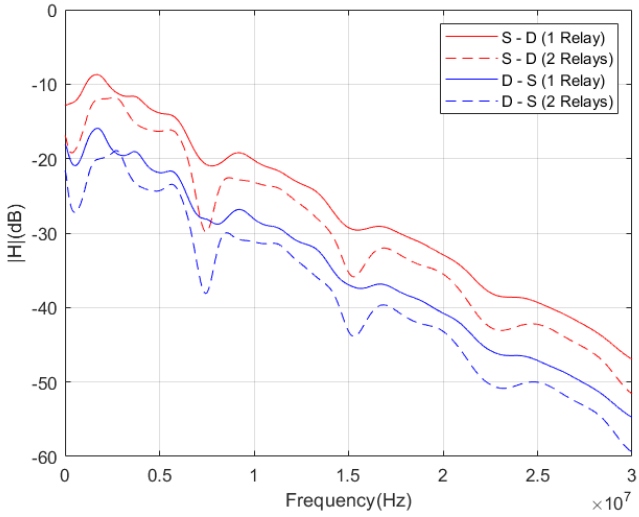

(d)

Fig. 9. Comparison between single-relay and two-relay two-way PLC system under four different topologies: (a) scenario 1, (b) scenario 2, (c) scenario 3, and (d) scenario 4.

For the first scenario, it can be seen that SYS A and SYS B have relatively the same forward CTFs, except that at certain frequencies, SYS B gives deeper attenuation. However, the backward CTFs of the two systems are relatively indifferentiable.

Similar to scenario 1, the results for scenario 2 show indistinguishable characteristics for SYS A and SYS B. It can also be seen that backward CTFs gives more deep attenuation at certain frequencies.

On the other hand, there are noticable differences, especially in high frequencies, between SYS A and SYS B in scenario 3. It can be seen that SYS B has better forward and backward CTFs at high frequencies. For the direcot links, it can be observed that SYS A provides better performance than SYS B. It can be understood by looking at the addition of branches which adds the channel attenuation.

IV. Conclusion

The CTFs of two-relay two-way PLC system has been investigated in this paper. The ABCD method has been applied to get the CTFs for both forward and backward channels. The composite CTFs for a certain link can be found by summing the respective CTFs of the constructive segments. We have also compared the CTFs between single-relay and two-relay two-way PLC systems. It has been shown that two-relay systems can be used when we want to make advantages of the number of relays as the CTFs for non-direct links are relatively similar or better than the single-relay PLC systems. On the other hand, if we mostly rely on the direct channel for data transmission, single-relay PLC system is preferred.

Acknowledgment

This work was supported by Fundamental Research Grant Scheme (FRGS) from Ministry of Higher Education Malaysia under FRGS/1/2016/TK04/CURTIN/02/1.

References

[1] K. M. Rabie, B. Adebisi, H. Gacanin, and S. Yarkan, "Energy-per-bit performance analysis of relay-assisted power line communication systems," *IEEE Trans. Green Commun. Netw.*, vol. 2, no. 2, pp. 360–368, 2018.

[2] I. Rubin, Y. Lin, and D. Kofman, "Optimal relay configuration for power line communication networks," *IEEE Trans. Commun.*, vol. 64, no. 1, pp. 130–140, 2016.

[3] G. Wei-chun, L. Huan-huan, Z. Hong-hao, G. Qiang, Z. Gui-ping, M. Yi-ling, and F. Li-na, "Research on communication technology of power monitoring system based on medium voltage power line carrier and low power wide area network," in *Proc. IEEE Conf. Energy Internet Energy System Integr. (EI2)*, Beijing, China, 2017, pp. 1–4.

[4] S. Gorshe, A. Raghavan, T. Starr, and S. Galli, *Power Line Communications*. Wiley Telecom, 2014.

[5] S. Galli, A. Scaglione, and Z. Wang, "For the grid and through the grid: The role of power line communications in the smart grid," in *Proc. of IEEE*, vol. 99, no. 6, Jun 2011, pp. 998–1027.

[6] J. Anatory, N. Theethayi, R. Thottappillil, M. M. Kissaka, and N. H. Mvungi, "An experimental validation for broadband power-line communication (bplc) model," *IEEE Trans. Power Del.*, vol. 23, no. 3, pp. 1380–1383, 2008.

[7] J. Anatory, N. Theethayi, and R. Thottappillil, "Power-line communication channel model for interconnected networks—part i: Two-conductor system," *IEEE Trans. Power Del.*, vol. 24, no. 1, pp. 118–123, 2009.

[8] A. M. Tonello and F. Versolatto, "Bottom-up statistical PLC channel modeling-—Part I: Random topology model and efficient transfer function computation," *IEEE Trans. Power Del.*, vol. 26, no. 2, pp. 891–898, Apr. 2011.

[9] B. Nikfar and A. J. Han Vinck, "Relay selection in cooperative power line communication: A multi-armed bandit approach," *J. Commun. Netw.*, vol. 19, no. 1, pp. 1–9, 2017.

[10] X. Wu, B. Zhu, and Y. Rong, "Channel model proposal for indoor relay–assisted power line communications," *IET Communications*, vol. 12, no. 10, pp. 1236–1244, Jun. 2018.

[11] R. K. Ahiadormey, P. Anokye, H. Jo, and K. Lee, "Performance analysis of two-way relaying in cooperative power line communications," *IEEE Access*, vol. 7, pp. 97 264–97 280, 2019.

[12] A. A. G. Liong, L. Gopal, F. H. Juwono, C. W. R. Chiong, and Y. Rong, "A channel model for three-node two-way relay-aided PLC systems," in *Proc. IEEE Int. Conf. on Signal Image Process. Appl. (ICSIPA)*, Kuala Lumpur, Malaysia, 2019, pp. 52–57.

[13] A. Dubey and R. K. Mallik, "PLC system performance with AF relaying," *IEEE Trans. Commun.*, vol. 63, no. 6, pp. 2337–2345, 2015.

[14] M. Rozman, A. Ikpehai, B. Adebisi, and K. M. Rabie, "Channel characterisation of cooperative relaying power line communication systems," in *Proc. IEEE Int. Symp. Commun. Syst. Netw. Digit. Signal Process. (CSNDSP)*, Prague, Czech Republic, July 2016, pp. 1–5.

[15] K. M. Rabie, B. Adebisi, H. Gacanin, G. Nauryzbayev, and A. Ikpehai, "Performance evaluation of multi-hop relaying over non-gaussian PLC channels," *J. Commun. Netw.*, vol. 19, no. 5, pp. 531–538, 2017.

[16] K. Kale and S. K. Patra, "Characterization of broadband power line channel," in *Proc. of Conf. Commun. Technol. (GCCT)*, Thuckalay, India, 2015, pp. 673–677.

[17] F. J. Canete, J. A. Cortes, L. Diez, and J. T. Entrambasaguas, "A channel model proposal for indoor power line communications," *IEEE Commun. Mag.*, vol. 49, no. 12, pp. 166–174, 2011.

[18] S. Galli and T. Banwell, "A novel approach to the modeling of the indoor power line channel-part ii: transfer function and its properties," *IEEE Trans. Power Del.*, vol. 20, no. 3, pp. 1869–1878, 2005.

[19] S. Liu, B. Gou, H. Li, and R. Kavasseri, "Power-line communication channel characteristics under transient model," *IEEE Trans. Power Del.*, vol. 29, no. 4, pp. 1701–1708, 2014.